

# Mechanism of Thioesterase-Catalyzed Chain Release in the Biosynthesis of the Polyether Antibiotic Nanchangmycin

Tiangang Liu,<sup>1,2</sup> Xin Lin,<sup>2</sup> Xiufen Zhou,<sup>1</sup> Zixin Deng,<sup>1,\*</sup> and David E. Cane<sup>2,\*</sup>

<sup>1</sup>Laboratory of Microbial Metabolism and School of Life Science and Biotechnology, Shanghai Jiaotong University, Shanghai 200030, China

<sup>2</sup>Department of Chemistry, Brown University, Box H, Providence, RI 02912-9108, USA

\*Correspondence: zxdeng@sjtu.edu.cn (Z.D.), david\_cane@brown.edu (D.E.C.)

DOI 10.1016/j.chembiol.2008.04.006

## SUMMARY

The polyketide backbone of the polyether ionophore antibiotic nanchangmycin (**1**) is assembled by a modular polyketide synthase in *Streptomyces nanchangensis* NS3226. The ACP-bound polyketide is thought to undergo a cascade of oxidative cyclizations to generate the characteristic polyether. Deletion of the glycosyl transferase gene *nanG5* resulted in accumulation of the corresponding nanchangmycin aglycone (**6**). The discrete thioesterase NanE exhibited a nearly 17-fold preference for hydrolysis of **4**, the *N*-acetyl-cysteamine (SNAC) thioester of nanchangmycin, over **7**, the corresponding SNAC derivative of the aglycone, consistent with NanE-catalyzed hydrolysis of ACP-bound nanchangmycin being the final step in the biosynthetic pathway. Site-directed mutagenesis established that Ser96, His261, and Asp120, the proposed components of the NanE catalytic triad, were all essential for thioesterase activity, while Trp97 was shown to influence the preference for polyether over polyketide substrates.

## INTRODUCTION

Polyether ionophores, produced primarily by *Actinomycetes*, have found widespread application in veterinary medicine and animal husbandry. For example, nanchangmycin (**1**) (also known as dianemycin), produced by *Streptomyces nanchangensis* NS3226, has been found to inhibit gram-positive bacteria, and can be used as a growth promotant in poultry and to cure coccidiosis in chickens (Sun et al., 2002; Figure 1). More recently, several polyethers, including monensin (**2**), salinomycin (**3**), nigericin, and nanchangmycin, have been shown to be active against drug-resistant strains of malaria (Gumila et al., 1997; Otoguro et al., 2001). A number of polyethers are also reported to inhibit the replication of human immunodeficiency virus (Nakamura et al., 1992).

Polyethers are branched, polyoxygenated polyketides, featuring two or more cyclic ether and acetal rings that are known to be derived from simple acetate, propionate, and butyrate building blocks. Classical incorporation experiments with [<sup>13</sup>C]-, [<sup>18</sup>O]-, and [<sup>2</sup>H]-labeled precursors with intact microbial cultures have

established the origin of the carbon skeleton and oxygen atoms of a variety of polyethers, and supported a general biosynthetic pathway in which an initially assembled, linear, unsaturated polyketide acid harboring double bonds all of *E*-geometry is oxidized to a polyepoxide that, in turn, undergoes a cascade cyclization to generate the characteristic polyether structure (Cane et al., 1981, 1982, 1983; Cane and Hubbard, 1987; Sood et al., 1984). A variety of late-stage modifications, including one or more methylation, hydroxylation, and glycosylation reactions, then yields the final polyether antibiotic.

Considerable insight into the detailed mechanism of polyether biosynthesis has come from the recent identification and sequencing of the individual biosynthetic gene clusters for the polyether antibiotics nanchangmycin (**1**) (Sun et al., 2003), monensin (**2**) (Oliynyk et al., 2003), and nigericin/abierixin (Harvey et al., 2007). The deduced genetic organization, which is similar for all three gene clusters, indicates that the polyketide backbone of each polyether is assembled by a large, modular polyketide synthase (PKS), highly analogous in sequence, organization, and deduced biochemical function to the well-characterized type I modular PKS proteins of macrolide polyketide biosynthesis (Fischbach and Walsh, 2006). Thus, the nanchangmycin gene cluster corresponding to *nanA1-nanA10* encodes a type I PKS harboring one loading module and 14 extension modules, corresponding to the 14 condensation steps required to assemble the linear pentadecaketide from a malonyl-CoA primer plus four malonyl-CoA and 10 methylmalonyl-CoA chain extension units (Sun et al., 2003; Figure 2). Similarly, the closely related monensin PKS consists of a malonyl-CoA-specific loading module plus one ethylmalonyl-CoA, four malonyl-CoA, and six methylmalonyl-CoA extension modules (Oliynyk et al., 2003). The predicted product of each such PKS is expected to be a branched-chain, all-*trans*-unsaturated fatty acid of the appropriate chain length (Cane et al., 1983; Oliynyk et al., 2003; Sun et al., 2003).

The next stage in the biosynthesis of nanchangmycin is thought to be the oxidative cyclization of the ACP-bound unsaturated polyketide, involving generation of the derived polyepoxide catalyzed by the *nanO* gene product, followed by enzyme-catalyzed polyepoxide cyclization, most likely mediated by NanI, resulting in the formation of the parent polyether (Cane et al., 1983; Sun et al., 2003; Figure 2). In the closely related *S. cinnamonensis*, the NanO homolog MonCI has been shown to catalyze the in vitro flavin-dependent epoxidation of model substrates (Oliynyk et al., 2003), while deletion of the *monBI* or *monBII* genes, which together correspond to the fusion gene

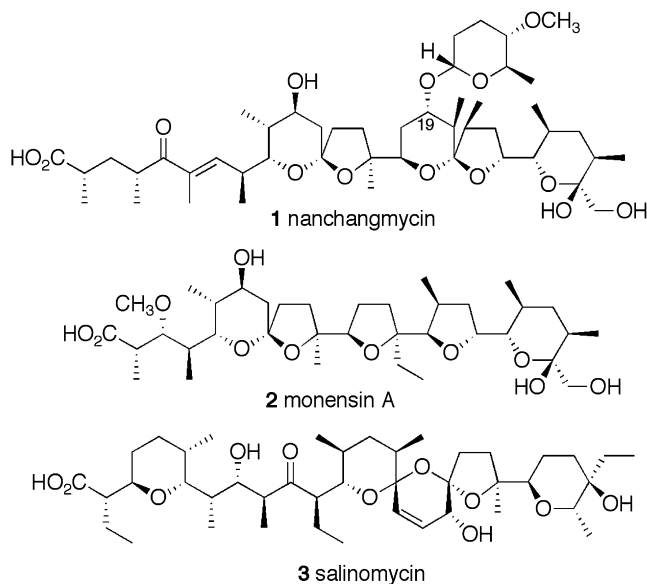


**Figure 1. Polyether Ionophores Nanchangmycin, 1, Monensin A, 2, and Salinomycin, 3**

*nanI* (Sun et al., 2003), has implicated the epoxide-hydrolase-like gene products in the cascade of polyepoxide cyclizations that generates the monensin polyether (Gallimore et al., 2006). Elegant experiments with mutants of *S. cinnamonensis* from which the *monCI* gene had been deleted have recently established that the monensin PKS produces the predicted full-length, branched-chain, polyoxygenated (*E,E,E*)-trienoic acid (Bhatt et al., 2005). The homologous *nigCI*, *nigBI*, and *nigBII* genes are thought to play completely analogous roles in the biosynthesis of nigericin/abierixin (Harvey et al., 2007).

The available evidence suggests that, in the formation of polyether ionophores, both the elaboration of the parent polyketide and the subsequent cascade of oxidative cyclizations take place exclusively on ACP-bound intermediates (Harvey et al., 2006, 2007; Liu et al., 2006; Sun et al., 2003). In a typical macrolide PKS, the initially formed polyketide product is directly released from the PKS as the derived macrolactone by a dedicated, *cis*-acting thioesterase (TE) domain that is fused to the C terminus of the most downstream module, immediately adjacent to the ACP domain (Khosla et al., 1999). By contrast, the nanchangmycin, monensin, and nigericin PKS clusters all lack such an intrinsic modular TE (Harvey et al., 2007; Oliynyk et al., 2003; Sun et al., 2003). Instead, the biosynthetic gene cluster for each polyether harbors a discrete type II TE gene that is responsible for the *in trans* hydrolytic release of the mature polyether from the cognate ACP domain. We have recently established that NanE is such a dedicated TE, and that it can hydrolyze **4**, the *N*-acetylcysteamine (SNAC) thioester of nanchangmycin, to nanchangmycin itself (Liu et al., 2006; Figure 3). Consistent with this result was the finding that a *nanE* deletion mutant of *S. nanchangensis* did not produce nanchangmycin or any other identifiable, related polyketide products. The highly homologous MonCII TE from *S. cinnamonensis* has independently been shown to catalyze the analogous hydrolysis of monensin-SNAC (**5**) to monensin (**2**) (Harvey et al., 2006), while NigCII is proposed to play a similar

role in nigericin biosynthesis, based on its 54% and 53% sequence similarity to NanE and MonCII, respectively (Harvey et al., 2007; Figure 4).

The final stages in the biosynthesis of nanchangmycin, monensin, and nigericin each involve a variety of late-stage chemical modifications of the polyether, including SAM-dependent formation of methyl ethers, P450-dependent hydroxylations, and, in the case of nanchangmycin, glycosylation of the C-19 hydroxyl by 4-*O*-methyl-L-rhodinose (Figure 2). Although some or all of these reactions may well take place prior to TE-catalyzed release of the mature polyether from the ACP, the precise sequence of biochemical events, including the relative timing of thioester hydrolysis and other late-stage chemical modifications, have not previously been established experimentally.

We report below the identification of the catalytic triad of the nanchangmycin TE, NanE, as well as investigations of the molecular basis for the substrate specificity of this TE. Deletion of the glycosyl transferase gene *nanG5* is also shown to abolish nanchangmycin biosynthesis, resulting in accumulation of small amounts of the corresponding nanchangmycin aglycone **6** that lacks the deoxy sugar. Taken together, these findings shed important light on the relative timing of late-stage modification and hydrolytic release of the polyether, and indicate strongly that NanE catalyzes the final step in the biosynthesis of nanchangmycin.

## RESULTS

### Identification of the NanE Catalytic Triad

Although comparison of the three polyether TEs indicates that they share a significant degree of mutual sequence similarity (NanE:MonCII, 49% identity, 59% similarity over 292 amino acids; NanE:NigCII, 47% identity, 60% similarity over 292 amino acids; Figure 4), the members of this group appear to be evolutionarily related only distantly to type I macrolide TEs, such as the TE domains of the 6-deoxyerythronolide B synthase (DEBS) and picromycin synthase (PICS) (Liu et al., 2006). The presumptive active site nucleophile serine in all of these TEs is typically found within the consensus sequence GX SXG, in spite of wide global sequence variations. Thus, Ser96 of NanE is found within a conserved GHSWG motif homologous to the active site GH<sup>72</sup>SAG of DEBS TE (Tsai et al., 2001). Comparison of NanE with other representative  $\alpha/\beta$ -hydrolases by multiple sequence alignment, however, did not suggest clear candidates for the remaining His and Asp components of the active-site triad (Liu et al., 2006). We therefore used the Modbase protein structure prediction package (Pieper et al., 2006; <http://modbase.compbio.ucsf.edu/modbase-cgi/index.cgi>) to generate homology models for NanE, with two structurally characterized members of the  $\alpha/\beta$ -hydrolase superfamily, chloroperoxidase (PDB ID: 1A88; 20% sequence identity) and  $\alpha$ -amino acid ester hydrolase (PDB ID: 1NX9; 13.00% sequence identity) as model protein templates. Although both predicted raw models for NanE suggested that His261 and Asp120 should be the nearest His and Asp residues to the putative active-site Ser96, the amino acid ester hydrolase-based homology model suggested closer inter-residue distances for the presumptive components of the NanE catalytic triad (His261–Ser96: 3.5 Å; Asp120–His261: 4.2 Å) (see Figure S4 in the Supplemental Data available with this article

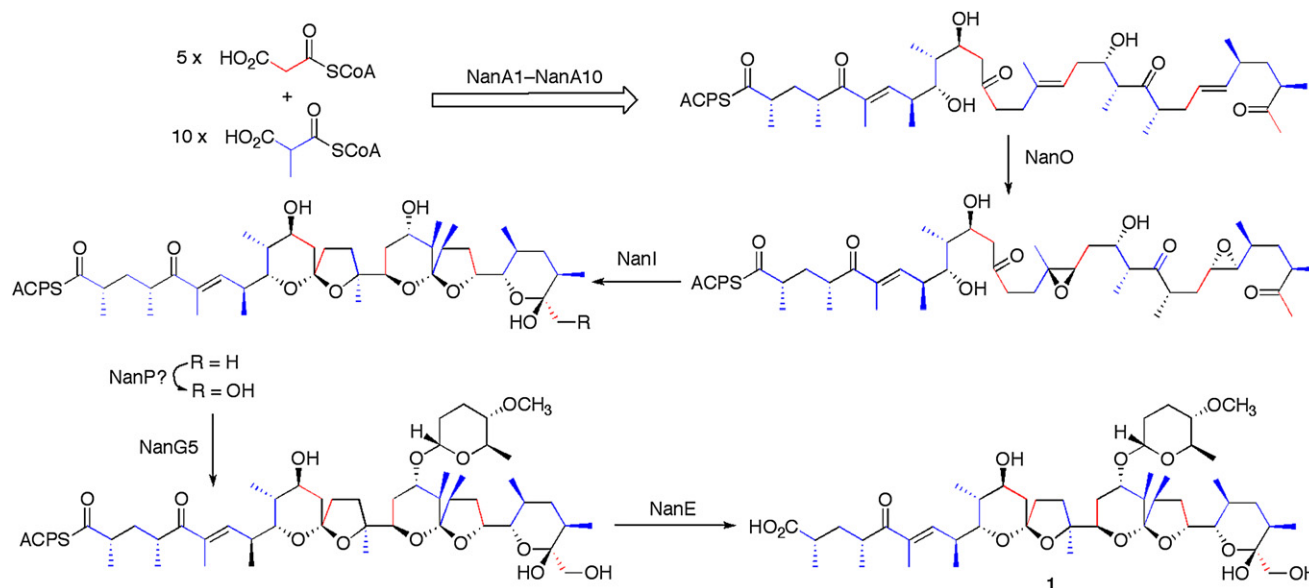


**Figure 2. Proposed Pathway of Nanchangmycin Biosynthesis in *S. nanchangensis* NS3226**

The parent polyketide is first assembled from a malonyl-CoA primer plus four malonyl-CoA and 10 methylmalonyl-CoA extension units, mediated by the 14 modules of the modular PKS NanA1–NanA10. The initially generated unsaturated pentadecaketide acyl-ACP ester is then thought to undergo NanO-catalyzed epoxidation, followed by a cascade of epoxide ring openings and acetalizations, catalyzed by NanI to generate the pentacyclic ether. Oxidation of the terminal methyl group by the P450 NanP generates the ACP-bound nanchangmycin aglycone, which is glycosylated at the C-19 hydroxyl under the control of NanG5, before final hydrolytic release by the NanE TE.

online). In this homology model, each of the three components of the catalytic triad resides on a loop connecting a  $\beta$  strand to a downstream  $\alpha$  helix. Interestingly, all three residues in the predicted catalytic triad of NanE correspond by sequence alignment to the previously proposed active-site residues of MonCII, Ser103, His265, and Asp127 that were predicted with an alternative  $\alpha/\beta$ -hydrolase model, aclacinomycin methylesterase (PBD ID: 1Q07; Harvey et al., 2006; Figure 4).

We tested the role of each of the predicted components of the NanE TE catalytic triad by generating the corresponding S96A, H261Q, and D120N mutants. Significantly, within the limits of experimental detection, all three variants were catalytically inactive. Thus, in contrast to wild-type NanE, none of these mutants was able to hydrolyze nanchangmycin-SNAC (4), even after extended incubation times with elevated concentrations of protein. These results establish that each of the three amino acids is essential for TE activity, consistent with their proposed role in the NanE catalytic triad.

#### Substrate Tolerance and Specificity of NanE

To investigate the relative timing of the NanE-catalyzed TE step in the overall course of nanchangmycin biosynthesis, we probed the substrate specificity of recombinant NanE toward the SNAC thioesters of a variety of polyethers, as well as a selection of typical polyketide TE substrates. We initially screened each SNAC-thioester substrate by overnight incubation with NanE, followed by analysis of the organic extract by MALDI-TOF. In this manner, it was found that, besides nanchangmycin-SNAC (4), NanE could also hydrolyze 7, the SNAC thioester of the nanchangmycin aglycone 6, and monensin-SNAC (5), but did not hydrolyze salinomycin-SNAC (8) (Figure 3). The requisite sample

of 6 was readily prepared by acid-catalyzed hydrolysis of nanchangmycin (1) to remove the deoxy sugar. Alternatively, we could isolate 6 directly from cultures of an *S. nanchangensis* mutant from which the relevant glycosyl transferase gene, *nanG5*, had been deleted, as described below (Figure 5). Among the polyketide substrates tested, NanE hydrolyzed the diketide (2*S*,3*R*)-2-methyl-3-hydroxypentanoyl-SNAC (9), as previously reported (Liu et al., 2006), as well as the corresponding 2-methyl-3-ketopentanoyl-SNAC (10). We have previously demonstrated that the branched-chain, polyoxygenated acyclic hexaketide *seco*-lactone-SNAC 11 can be efficiently lactonized by the type I TEs of both the picromycin and erythromycin synthases, PICS TE (Aldrich et al., 2005; He et al., 2006) and DEBS TE (He et al., 2006), while the corresponding *seco*-7-dihydroxylactone-SNAC 12 is hydrolyzed by each of these two TEs. By contrast, neither 11 nor 12 underwent either lactonization or hydrolysis when incubated with the nanchangmycin TE, NanE, suggesting that NanE has a marked preference for polyether substrates.

We next determined the steady-state kinetic parameters for each of the active substrates. Nanchangmycin-SNAC (4) was the preferred substrate for the NanE TE, with a  $k_{\text{cat}}/K_m$  17-fold that of the nanchangmycin aglycone-SNAC (7) and 36-fold that of monensin-SNAC (5) (Table 1). The observed differences in  $k_{\text{cat}}/K_m$  primarily reflect 9-fold and 11-fold increases in the  $K_m$  values for 7 (220  $\mu\text{M}$ ) and 5 (270  $\mu\text{M}$ ), respectively, compared to the  $K_m$  of 24  $\mu\text{M}$  for nanchangmycin-SNAC (4), with only modest 2- and 3-fold reductions in  $k_{\text{cat}}$ . Interestingly, although the two simple diketide substrates 9 and 10 exhibited  $k_{\text{cat}}$  values that were actually 60- and 1450-fold greater than that of nanchangmycin-SNAC, the higher turnover numbers were

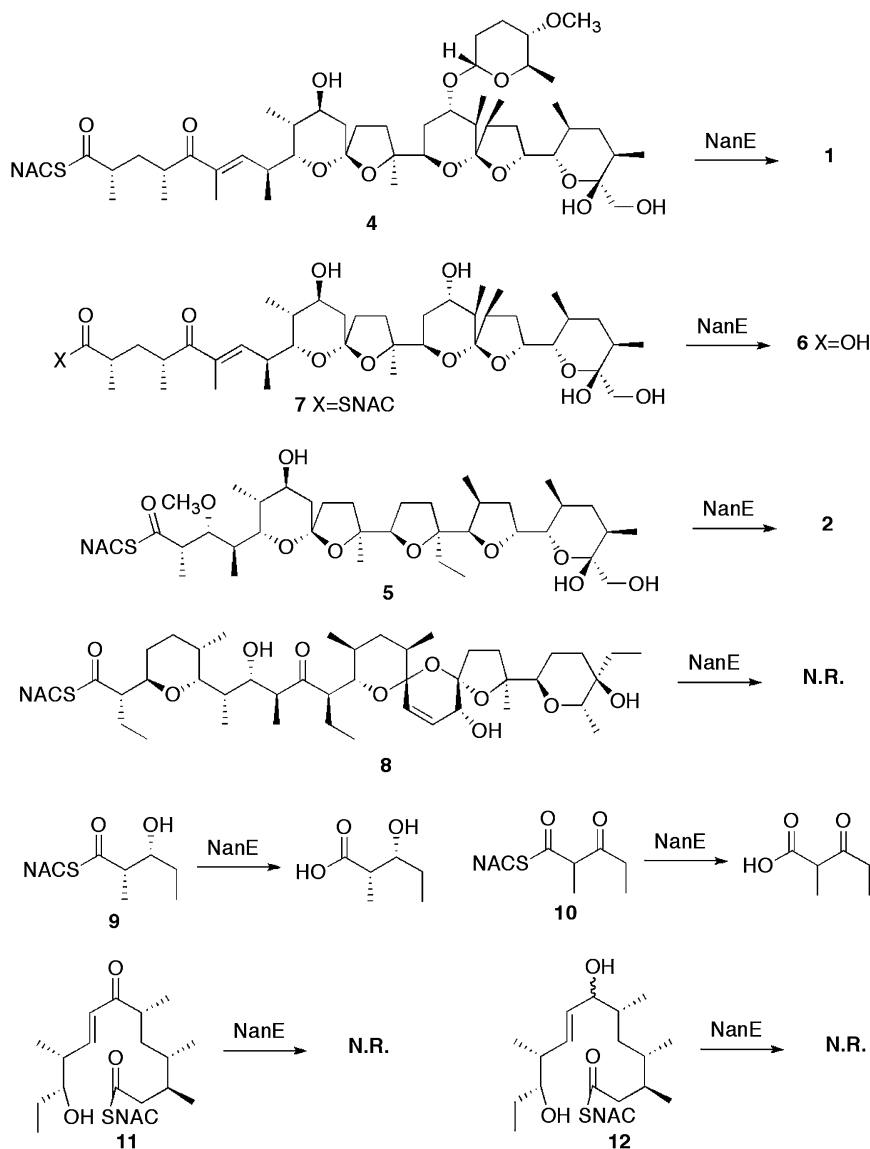


**Figure 3. Hydrolysis of Polyether and Polyketide-SNAC Substrates by the NanE TE**  
N.R. indicates no reaction.

also retained TE activity for the ketodiketide-SNAC **10**, although the activity was somewhat reduced compared with wild-type NanE.

### Generation of the *nanG5* Glycosyl Transferase Mutant and Isolation of Nanchangmycin Aglycone

The nanchangmycin biosynthetic gene cluster harbors three putative glycosyl transferase genes, *nanG5*, *nanG6*, and *nanG7* (Sun et al., 2003). Simultaneous deletion of both *nanG6* and *nanG7* did not suppress nanchangmycin production (data not shown). We therefore turned our attention to *nanG5*. Sequence analysis indicated that *nanG5* carries its own promoter and is transcribed in the direction opposite to that of both of its flanking genes, *nanA6* and *nanM* (Figure 5). RT-PCR also established that *nanG5* is constitutively expressed (see the Supplemental Data). To delete the chromosomal copy of *nanG5* from wild-type *S. nanchangensis* NS3226, we used PCR-targeted mutagenesis (Kieser et al., 2000; Sun et al., 2002; Figure 5). After two rounds of homologous recombination and selection, two identical thiostreptone-sensitive (Thio<sup>S</sup>), apramycin-resistant (Apra<sup>R</sup>) *nanG5* deletion mutants were isolated: *S. nanchangensis* LTΔ*nanG5*-4 and LTΔ*nanG5*-19.

Surface cultures of each deletion mutant failed to produce nanchangmycin,

offset by 2000- to 3000-fold increases in  $K_m$ . This resulted in net  $k_{cat}/K_m$  specificity constants that were actually only 3% and 55%, respectively, that of nanchangmycin-SNAC (**4**), the analog of the presumed natural ACP-bound polyether substrate.

Comparison of the GHSWG consensus sequence flanking the active-site serine residues of the polyether TEs NanE, MonCII, and NigCII with the conserved GHSAG motif of modular polyketide TEs typified by DEBS TE and PICS TE (Liu et al., 2006) reveals an intriguing difference, with the modular type I TEs carrying an Ala residue downstream of the active-site Ser compared with a Trp at the same position in all three type II polyether TEs. To explore the possible influence of this active-site Trp on the substrate specificity of NanE, we generated the corresponding W97A mutant. Interestingly, the NanE W97A mutant lost the ability to hydrolyze the native substrate nanchangmycin-SNAC (**4**), but it was in fact 12-times more active toward diketide-SNAC **9** than wild-type NanE, an activity level comparable to that of DEBS TE toward the same substrate. The W97A NanE mutant

as determined by both HPLC and MALDI-TOF MS analysis of the organic extracts. Both deletion mutants were observed, however, to produce a novel metabolite, which was isolated and purified from the extracts of *S. nanchangensis* LTΔ*nanG5*-4 and found to have  $m/z$  ( $M+Na^+$ ) 761.5, corresponding to the expected mass of nanchangmycin aglycone (**6**) (Figure 5C). The yield of **6** per liter of *S. nanchangensis* LTΔ*nanG5*-4 was ~1% that of nanchangmycin generated by the wild-type NS3226 strain. Preparative-scale incubations followed by extraction, silica gel chromatography, and preparative HPLC purification yielded ~2 mg of **6** from 8 l of solid culture. The structure of **6** was fully confirmed by detailed 1D and 2D  $^1H$ ,  $^{13}C$  NMR analysis (see the Supplemental Data), and high-resolution MS, as well as by direct comparison with a synthetic sample obtained by hydrolysis of the parent nanchangmycin. Both the  $^1H$  and  $^{13}C$  spectra of the aglycone **6** closely resembled the corresponding spectra of the polyether backbone of nanchangmycin (**1**), except for changes associated with the removal of the



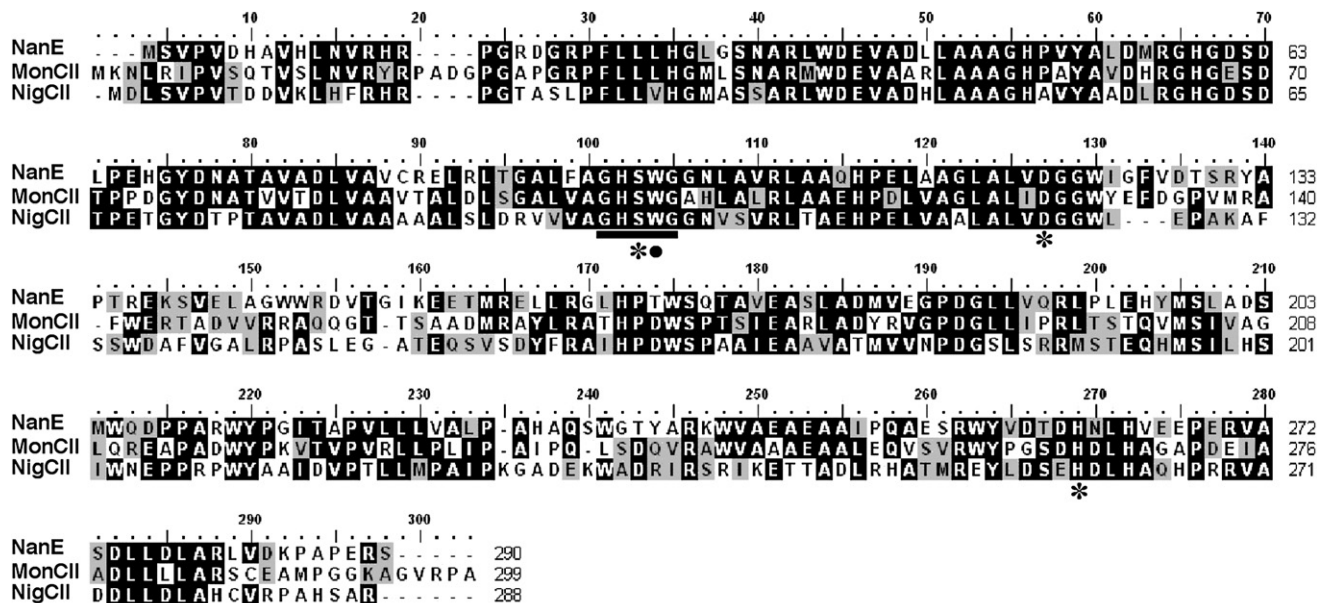


**Figure 4. Sequence Comparison of the Type II TEs Encoded by the Nanchangmycin, Monensin, and Nigericin Biosynthetic Gene Clusters**

The asterisk indicates the Ser/His/Asp catalytic triad, the solid line designates the conserved GX SXG motif surrounding the active site Ser, and the black dot marks the conserved Trp residue in this motif that corresponds to an Ala in the type I TEs of polyketide biosynthesis. MonCII = monensin; NanE = nanchangmycin; NigCII = nigericin.

4-*O*-methyl-L-rhodinose. Aside from the complete absence of resonances corresponding to the deoxy sugar, the  $^{13}\text{C}$  NMR signal for C-19 of **6** appeared at 71.7 ppm, an upfield shift of  $-7.7$  ppm relative to nanchangmycin, consistent with the removal of the deoxy sugar. At the same time, the signals for the adjacent C-18 methylene and C-20 methine carbons in **6** exhibited  $+3.1$  ppm and  $+5.8$  ppm downfield shifts, respectively, relative to the corresponding  $^{13}\text{C}$  NMR signals in **1**. Similarly, the  $^1\text{H}$  NMR signal at  $\delta$  3.73 for the H-19 proton of **6** showed COSY cross-peaks to adjacent H-18 and H-20 protons at  $\delta$  1.56 and  $\delta$  1.91, respectively, as well as to the C-19 hydroxyl proton at  $\delta$  4.21.

## DISCUSSION

The primary sequence of the nanchangmycin TE NanE is closely related to that of the monensin (MonCII) and nigericin (NigCII) TEs, with which it shares a common biochemical function (Figure 4). In spite of only very limited overall sequence similarity between each of these three type II TEs and more distantly related modular PKS TE domains, such as DEBS and PICS TE (Liu et al., 2006), the structures of the three polyether TEs can all be fit to a protein homology model corresponding to the  $\alpha/\beta$ -hydrolase superfamily. Interestingly this same superfamily is also distantly related to both DEBS and PICS TE, for which the actual structures are already known (Tsai et al., 2001, 2002), in spite of considerable differences in the predicted three-dimensional structures of the type II polyether TEs (Liu et al., 2006). We have used site-directed mutagenesis to identify the catalytic triad of NanE, Ser96, His261, and Asp120, each of which is shown to be essential to TE activity. These three NanE residues

also align with the independently predicted catalytic triad of MonCII, Ser103, His265, and Asp127 (Harvey et al., 2006).

In the biosynthesis of macrolide and related polyketides, the full-length polyketide chain is released, usually as the macrolactone aglycone, from the modular PKS by the action of a dedicated, *cis*-acting TE domain located at the C terminus of the furthest downstream module, immediately adjacent to the ACP domain to which the mature polyketide chain is tethered. Type I TEs, which catalyze the lactonization and release of their polyketide substrates from the modular PKS, must bind and fold their ACP-bound substrates so as to position the nucleophilic distal hydroxyl group within bonding distance of the acylthioester moiety (Akey et al., 2006). Most, if not all, subsequent modifications, including P450-catalyzed hydroxylation and the addition of various deoxy sugars, then take place on protein-free, macrolide polyketide intermediates. By contrast, in the biosynthesis of polyethers, some or all of the modifications of the parent unsaturated polyketide, including the cascade of oxidative cyclizations that generates the characteristic polyether as well as subsequent, late-stage modifications, are thought to take place while the polyether precursors and intermediates are still tethered to an ACP. Unlike the type I TE domains of typical modular PKSs, the type II NanE TE, as well as the closely related MonCII and NigCII TEs (Harvey et al., 2006, 2007), are each discrete proteins that catalyze the hydrolytic release, rather than the lactonization, of their cognate substrates. Although the precise structures of these natural substrates, as well as the identity of the specific ACP domains to which those substrates are covalently tethered, have been obscure, strong circumstantial evidence has suggested that the epoxidation-cyclization cascades that generate nanchangmycin and monensin precede hydrolytic release of the free polyether. Prior to this work, the order of late-stage

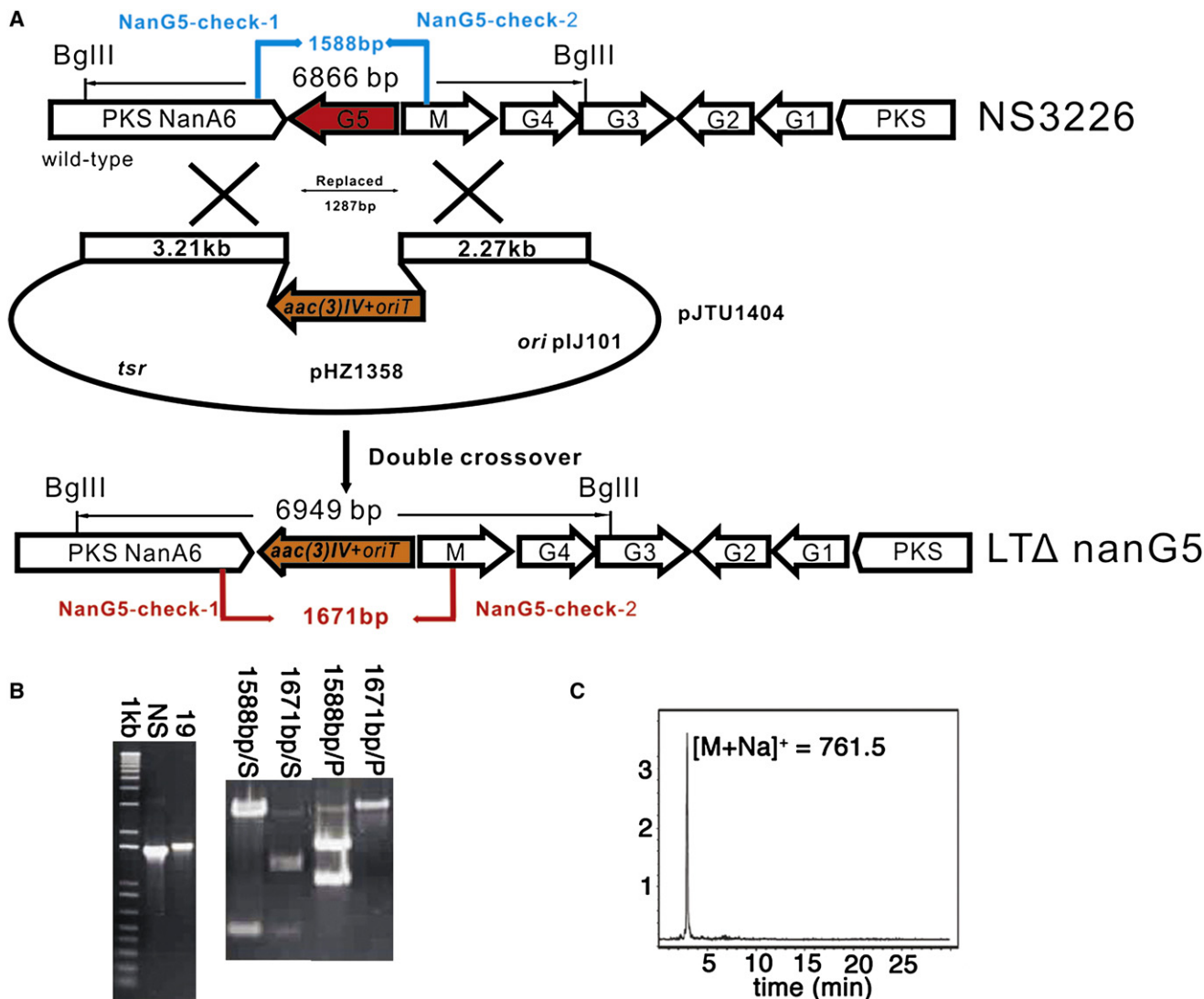


**Figure 5. Deletion of the *nanG5* Glycosyl Transferase Gene of *S. nanchangensis* NS3226 Abolishes Nanchangmycin Production and Leads to Accumulation of the Nanchangmycin Aglycone, 6, in the Deletion Mutant *S. nanchangensis* LTΔ*nanG5***

(A) Replacement of *nanG5* by the apramycin resistance gene cassette *aac(3)IV* by PCR-directed mutagenesis and homologous recombination to generate *S. nanchangensis* LTΔ*nanG5*.

(B) The genomic DNA in the LTΔ*nanG5*-19 mutant was checked by PCR amplification with primers NanG5-check-1 and NanG5-check-2. In the wild-type, the PCR product is 1,588 bp, while in the mutant the PCR product is 1,671 bp. Digestion of each fragment with *Sac*I (S) and *Pvu*II (P) gave fragments of different sizes.

(C) LC-ESI-MS of nanchangmycin aglycone (6), retention time of 2.89 min isolated from *S. nanchangensis* LTΔ*nanG5*-4.

glycosylations, P450-catalyzed hydroxylations, and SAM-dependent formation of methyl ethers had not yet been established, nor had the timing of TE-catalyzed hydrolysis relative to these transformations been previously determined. Production of nanchangmycin aglycone 6, lacking only the deoxy sugar 4-O-methyl-L-rhodinose, by the *S. nanchangensis* LTΔ*nanG5*-4 mutant strongly suggests that glycosylation is the penultimate chemical step preceding TE-catalyzed release of the finished nanchangmycin. The release of the free aglycone by the *nanG5* mutant presumably results from the adventitious action of the NanE TE, with the empirically reduced yield of 6 possibly reflecting the fact that the ACP-bound aglycone thioester is a considerably poorer substrate for NanE. Although these observations

alone cannot rule out the possibility of aberrant C-30 hydroxylation, the complete absence of the corresponding 30-deoxy-aglycone in the organic extract of *S. nanchangensis* LTΔ*nanG5*-4 or LTΔ*nanG5*-19 suggests that C-30 hydroxylation most likely precedes both C-19 glycosylation and NanE-catalyzed TE hydrolysis (Figure 2).

NanE, while broadly tolerant of a variety of substrates, is seen to strongly prefer the natural polyether substrate nanchangmycin-SNAC 4 over both simple diketide substrates, such as diketide 9, and more complex, branched-chain polyketide substrates, such as 11, the *seco*-acid-SNAC thioester substrate of PICS TE (He et al., 2006; Table 1). These preferences largely reflect substantial 1000- to 2000-fold differences in relative  $K_m$

**Table 1. Steady-State Kinetic Parameters for Hydrolysis of Polyether- and Polyketide-SNAC Esters by Wild-Type and Mutant TEs**

Enzyme	Substrate	$k_{\text{cat}}$ ( $\text{min}^{-1}$ )	$K_{\text{m}}$ (mM)	$k_{\text{cat}}/K_{\text{m}}$ ( $\text{M}^{-1} \text{s}^{-1}$ )	$k_{\text{cat}}/K_{\text{m}}$ (rel)
NanE	<b>4</b>	$0.0036 \pm 0.0001$	$0.024 \pm 0.002$	$2.5 \pm 0.2$	100
	<b>7</b>	$0.0020 \pm 0.0002$	$0.220 \pm 0.035$	$0.15 \pm 0.03$	6
	<b>5</b>	$0.00115 \pm 0.00003$	$0.270 \pm 0.010$	$0.070 \pm 0.004$	3
	<b>9</b>	$0.210 \pm 0.006$	$44 \pm 3$	$0.080 \pm 0.008$	3
	<b>10</b>	$5.2 \pm 1.0$	$64 \pm 12$	$1.35 \pm 0.4$	54
NanE W97A	<b>9</b>	$0.101 \pm 0.001$	$1.7 \pm 0.1$	$0.99 \pm 0.07$	40
	<b>10</b>	$0.66 \pm 0.01$	$31 \pm 1$	$0.35 \pm 0.01$	14
DEBS TE <sup>a</sup>	<b>9</b>	$0.68 \pm 0.16$	$9.6 \pm 4.5$	$1.2 \pm 0.6$	48
	<b>10</b>	n.d.	n.d.	$8.8 \pm 0.9$	350

n.d. = not determined.

<sup>a</sup>Data from Tsai et al., 2002.

between the two classes of substrates. These observations lend strong support to a biosynthetic model in which formation of the ACP-bound polyether precedes NanE-catalyzed product release. Furthermore, the finding that NanE has a 17-fold preference, as measured by relative  $k_{\text{cat}}/K_{\text{m}}$ , for nanchangmycin-SNAC (**4**) over the corresponding nanchangmycin aglycone-SNAC (**7**) is consistent with a biosynthetic pathway in which glycosylation with 4-O-methyl-L-rhodinose precedes release of the mature nanchangmycin from the ACP, leading to the conclusion that NanE-catalyzed hydrolysis is the final step in nanchangmycin biosynthesis. The fact that monensin-SNAC (**5**) is a poor substrate for NanE ( $k_{\text{cat}}/K_{\text{m}}$  36-fold lower than **4**), yet still has a 270  $\mu\text{M}$   $K_{\text{m}}$ , 100-fold tighter than that of the simple diketide substrates, underscores the selectivity of NanE for both its cognate polyether backbone and the glycosylation state of its substrate.

Interestingly, in spite of the precision of the experimentally determined steady-state kinetic parameters for all three polyether-SNAC derivatives, the apparent  $k_{\text{cat}}$  of  $3.6 \pm 1 \times 10^{-3} \text{ min}^{-1}$  for **4** appears to be well below the expected *in vivo* rate for the ACP-bound substrate. For example, the observed turnover rate of  $0.2 \text{ hr}^{-1}$  for the -SNAC ester would require more than 30–40 mg of NanE protein (MW, 31,855 Da) per liter of *S. nanchangensis* NS3226 culture in order to account for the observed production of  $\sim 0.2 \mu\text{mol/hr}$  of nanchangmycin per liter of solid culture (25 mg over 5–7 d). By comparison, the  $k_{\text{cat}}$  values of 1–10  $\text{min}^{-1}$  for typical PKS modules and TE domains are 1000 times faster than that determined for NanE acting on the nanchangmycin-SNAC substrate. Although, for many PKSs and fatty acid synthases, use of the SNAC analog as a surrogate for the ACP has only minor effect on the observed  $k_{\text{cat}}$ , resulting primarily in increases in the apparent  $K_{\text{m}}$ , there is at least one known example of depression of the apparent  $k_{\text{cat}}$  as well. Thus the  $k_{\text{cat}}$  for processing diketide-SNAC **9** by DEBS module 5 is only 2% that for the corresponding diketide-ACP4 conjugate (Tsuiji et al., 2001). We therefore speculate that NanE may also have a strong preference for the specific ACP to which the mature nanchangmycin polyether is naturally tethered. Unlike the type I TE domains of modular PKSs, NanE is a discrete protein and, therefore, must somehow be selective for its specific polyether-ACP conjugate substrate. There is some evidence that discrete type II acyl carrier proteins, MonACPX and NigACPX, may act as the carriers of the full-length polyketide

acyl chain during the oxidative cyclization and additional late-stage modifications in the monensin and nigericin biosynthetic pathways, respectively (Harvey et al., 2007; Oliynyk et al., 2003). The identity of the corresponding ACP that might serve as the physiological carrier for the full-length polyketide and derived nanchangmycin polyether intermediates is not yet known, although the ACP domain of nanchangmycin synthase module 14 or the discrete ACP13 encoded by the *nanA10* gene are plausible candidates.

Importantly, in the study by Tsuiji et al. (2001), the use of the ACP derivatives had little effect on the relative values of the measured  $k_{\text{cat}}/K_{\text{m}}$  for the four diastereomers of the diketide thioester. Whether or not the nanchangmycin ACP influences the absolute values of the steady-state kinetic parameters for the various NanE substrates that were examined, it is unlikely that the relative values of the  $k_{\text{cat}}/K_{\text{m}}$  specificity constants for these substrates are significantly perturbed. Comparison of the relative values therefore provides useful insights into the intrinsic substrate specificity of this TE. Indeed, NanE shows a strong preference for polyether over branched-chain polyketide thioesters. Interestingly, the NanE W97A mutant, in which the polyether TE consensus sequence GHSWG harboring the active-site Ser had been replaced by the GHSAG consensus sequence of the DEBS and PICS TEs, showed a 12-fold increase in  $k_{\text{cat}}/K_{\text{m}}$  for hydrolysis of diketide **9**, nearly equal to the efficiency of processing by DEBS TE (Lu et al., 2002), while losing all hydrolytic activity toward the natural polyether substrate **4**.

Of the four polyether-SNAC thioesters that we examined, nanchangmycin-SNAC (**4**) was by far the best substrate, with a 17-fold preference over the next-best candidate, nanchangmycin aglycone-SNAC (**6**). Taken together with the complete abolition of nanchangmycin production by the glycosyl transferase deletion mutants, *S. nanchangensis* LT $\Delta$ nanG5-4 and LT $\Delta$ nanG5-19, as well as the concomitant 100-fold reduction in the yield of polyether aglycone in this mutant, there is strong evidence that the final step in nanchangmycin biosynthesis is release of the mature polyether by NanE-catalyzed hydrolysis of the nanchangmycin-SACP thioester.

## SIGNIFICANCE

**The polyketide backbones of both macrolide and polyether antibiotics are each assembled by closely related, large,**

multifunctional, modular polyketide synthases. The initially generated polyketides in both cases also typically undergo a variety of similar late-stage modifications, including oxidation, methylation, and glycosylation reactions. In spite of these overall similarities, there are a number of important biochemical differences between the biosynthetic pathways. While the parent macrolide polyketide is typically released from the ACP domain of the furthest downstream module, and lactonized by an integrated, type I TE domain located at the C terminus of this last module, prior to all further modifications, all the late-stage modifications of polyether biosynthesis, including the characteristic epoxidation-cyclization cascade, appear to take place while the full-length polyketide is still tethered to an ACP domain. A combination of both biochemical and molecular genetic experiments strongly indicates that the penultimate step in the biosynthesis of the polyether nanchangmycin is the attachment of the deoxy sugar 4-O-methyl-L-rhodinose to the C-19 hydroxyl group of the ACP-bound polyether aglycone, catalyzed by the glycosylase NanG5. The type II thioesterase NanE catalyzes the final step in the biosynthetic pathway, the hydrolytic release of the fully modified polyether from an as-yet unidentified ACP domain.

## EXPERIMENTAL PROCEDURES

### Materials and Methods

Reagents for kinetic assays and chemical synthesis were purchased from Sigma-Aldrich Chemical Co., and were of the highest grade available. (2*S*,3*R*)-2-Methyl-3-hydroxypentanoyl-SNAC (**9**) and 2-methyl-3-ketopentanoyl-SNAC (**10**) were prepared as previously described (Lu et al., 2002). The *seco*-10-deoxymethynolide-SNAC (**11**) and *seco*-7-dihydro-10-deoxymethynolide-SNAC (**12**) were a kind gift from Weiguo He (He et al., 2006). Culture medium components were obtained from Difco. Restriction enzymes and T4 DNA ligase were purchased from Promega. Oligonucleotide primers were obtained from Integrated DNA Technologies. DNA sequencing of PCR products and plasmids was performed by the U.C. Davis Sequencing Facility (Davis, CA). MALDI-TOF analysis was carried out on an Applied Biosystems Voyager-DE Pro spectrometer.

### Bacterial Strains, Vectors

Wild-type *S. nanchangensis* NS3226 was used for production of nanchangmycin as well as generation of mutant strains by targeted gene replacement. *Escherichia coli* XL1-blue was the host for cloning DNA fragments. *E. coli* ET12567, carrying RP4 derivative pUZ8002 (*recF dam dcm Cml<sup>R</sup> Str<sup>R</sup> Tet<sup>R</sup> Km<sup>R</sup>*) (Gust et al., 2003; Kieser et al., 2000), was used as donor for intergeneric conjugation. *E. coli* BW25113, carrying pJ790, was used for recombination during PCR-targeted gene replacement. The plasmid pHZ1358 (Gust et al., 2003; Kieser et al., 2000) was used for conjugative transfer and screening for double crossovers.

### Site-Directed Mutagenesis of NanE

Plasmid pJTU1373 (Liu et al., 2006), in which the *nanE* gene had been subcloned into *Nde*I- and *Hind*III-digested pET28a (Novagen), was used as the template for site-directed mutagenesis. Mutants were prepared with the QuikChange Site-Directed Mutagenesis Kit (Stratagene). The individual primer pairs are listed in the Supplemental Data. The resultant plasmids were isolated with a QIAGEN kit, and were sequenced to confirm the sequence of the mutant gene.

### Expression and Purification of Wild-Type and Mutant NanE

Plasmids harboring *nanE* mutants were transformed into *E. coli* BL21 (DE3)/pLysS. All the encoded proteins had an N-terminal His<sub>6</sub> tag. Expression procedures were the same for wild-type NanE and for each mutant. Each

*E. coli* BL21(DE3)/pLysS colony was grown overnight at 37°C in 5 ml of LB culture, which was then used to inoculate fresh LB medium (500 ml) in a 2 l flask supplemented with 30 µg/ml kanamycin and 25 µg/ml chloramphenicol to maintain the plasmids. The protein was induced at an OD<sub>600</sub> of 0.8 with 0.6 mM IPTG, and incubation was continued for 12 hr at 24°C (room temperature).

All protein purification procedures were performed at 4°C. The cells from 2 l of culture were harvested by centrifugation at 4000 × g (15 min) and suspended in 30 ml of buffer A for FPLC (50 mM Tris-HCl, 150 mM NaCl [pH 7.5]). The cells were disrupted by passage twice through a French press at 600 psi, with removal of the cell debris by centrifugation at 17,200 × g (2 × 30 min). The wild-type protein and W97A mutant were purified by Ni-NTA column, anion exchange, and gel filtration FPLC. The S96A, D120N, and H261Q mutants were purified on a 5 ml HisTrap HP Ni-NTA column by FPLC. The column was washed with 30 ml (6 column volumes) buffer A, and then the protein supernatant from the crude cell lysate was loaded onto the column by autoinjection at a flow rate of 1.5 ml/min. The column was then washed with 20 ml of buffer A (4 column volumes) followed by a 0%–100% linear gradient of buffer B (50 mM Tris-HCl, 150 mM NaCl, 250 mM imidazole [pH 7.5]) over 100 ml (20 column volumes), and then a 20 ml 100% buffer B wash (4 column volumes). The wild-type NanE and each of the N-terminal His-tag mutants eluted at 45%–60% of buffer B. The purity of protein (~70%) was checked by SDS-PAGE. The protein was concentrated with a Centricon-10 concentrator (Amicon) to 2.5 ml and exchanged into Buffer C (20 mM Tris-HCl, 10 mM NaCl [pH 8.0]) with a PD-10 column (Pharmacia).

The protein was diluted to 3.5 ml, and this sample was directly autoinjected onto the FPLC and purified by anion exchange on HiTrap 16/10 Q/FF. The column was washed with 20 ml buffer C (1 column volume), and eluted with a linear gradient of buffer D (20 mM Tris-HCl, 1 M NaCl [pH 8.0]): 0%–30% buffer D for 20 ml (1 column volume); 30%–50% buffer D for 40 ml (2 column volume); 50%–100% buffer D for 20 ml (1 column volume); and 100% buffer D for 20 ml (1 column volume). The wild-type NanE and W97A mutant eluted from 35% to 40% of buffer D. The purity of protein was ~85%, based on SDS-PAGE. The target protein was concentrated to 2 ml and further purified by gel filtration FPLC on a Superdex 200. The column was equilibrated by washing with 240 ml (2 column volumes) of buffer E (50 mM phosphate buffer [pH 8.0]) before injection. The wild-type protein and mutant both behaved as dimers, each eluting at ~80 ml. The final purity of the wild-type NanE and its mutant was ~95%, as determined by SDS-PAGE.

### Knockout of Glycotransferase *nanG5* by PCR Targeting

PCR-targeted mutagenesis was used to replace the chromosomal sequence for *nanG5*, carried in an *S. nanchangensis* cosmid, by a selectable apramycin marker generated by PCR, with primers with 39-nt homology extensions (Gust et al., 2003). A 6866 bp BglIII fragment from *S. nanchangensis* cosmid 11A8 containing *nanG5* and *nanM* flanked by partials of *nanA6* and *nanG4* was first cloned into the BamHI site of the *Streptomyces-E. coli* shuttle cosmid vector, pHZ1358, carrying *oriT*, furnishing plasmid pJTU1403. The inclusion of *oriT* (RK2) in the disruption cassette allowed selection of the mutant following introduction of the PCR-targeted cosmid DNA into the *Streptomyces* host by conjugation. After PCR amplification with primers NanG5-1 and NanG5-2, the resulting PCR amplicon was used to replace 1287 bp of *nanG5* by double homologous recombination in *E. coli* BW25113/pJ790 so as to furnish plasmid pJTU1404. pJTU1404 was introduced into *S. nanchangensis* strain NS3226 by conjugation from the nonmethylating *E. coli* donor strain ET12567::pUZ8002. Thio<sup>S</sup> and Apra<sup>R</sup> colonies were counter selected from the initial Thio<sup>S</sup> exconjugants after one round of nonselective growth. Two Thio<sup>S</sup>Apra<sup>R</sup> exconjugants, deletion mutants *S. nanchangensis* LTΔ*nanG5*-4 and LTΔ*nanG5*-19, were confirmed to be identical by PCR amplification with the primers NanG5-check-1 and NanG5-check-2, followed by further sequencing to confirm the desired deletion.

### Isolation of Nanchangmycin Aglycone, **6**, from the *nanG5* Deletion Mutant

Nanchangmycin aglycone (**6**) was prepared by extraction of 8 l of 7-day-old solid SFM (20 g soy flour, 20 g D-mannitol, 16 g agar in tap water to 1 l) cultures of *S. nanchangensis* LTΔ*nanG5*-4 with 4 l of methanol for 8 hr, followed by centrifugation at 17,200 × g for 10 min. After drying of the supernatant over



Na<sub>2</sub>SO<sub>4</sub> and evaporation of the solvent, the residual yellow oil was dissolved in 4 ml of chloroform. The crude sample was purified by flash column chromatography on silica gel (particle size, 0.040–0.063 mm) with a linear gradient of chloroform:methanol. The nanchangmycin aglycone (**6**) eluted at 6%–8% methanol. The concentrated sample was dissolved in acetonitrile and further purified by preparative RP-HPLC (100 × 30 mm Phenomenex C18 Axia preparative column with a linear gradient program of acetonitrile/H<sub>2</sub>O:80% acetonitrile over 2 min, 80%–85% over 3 min, 85%–90% over 3 min, 90%–95% over 2 min, 95%–100% over 5 min, and constant 100% acetonitrile over 15 min at a flow rate of 15 ml/min. The elution of nanchangmycin aglycone (retention time = 12 min) was monitored at 234 nm. HR-FABMS: *m/z* 761.4480 (calculated for C<sub>40</sub>H<sub>66</sub>O<sub>12</sub>Na 761.4452).

#### Semisynthesis of Nanchangmycin Aglycone, **6**

Nanchangmycin (**1**, 15 mg) was dissolved in 500 μl of acetonitrile, 400 μl of acetic acid, and 100 μl of water, and the solution was incubated at 50°C for 1.5 hr (Williams and Kissel, 1998). After adjustment of the pH to ~5 with saturated NaHCO<sub>3</sub>, the acetonitrile was removed under reduced pressure, and the organic product was extracted into 3 × 10 ml of EtOAc. After back extraction with saturated aqueous NaCl, the EtOAc was evaporated and the residue dissolved in 3 × 300 μl acetonitrile, filtered through a 2 μm filter, and purified by preparative RP-HPLC, as described above, to yield 6 mg of purified nanchangmycin aglycone (**6**). See Table S1 for <sup>1</sup>H and <sup>13</sup>C NMR data on **6** and **1**.

#### Polyether-SNAC Esters

Each polyether (0.03 mmol), diphenylphosphoryl azide (0.06 mmol), and Et<sub>3</sub>N (0.12 mmol) were added to 2 ml of CH<sub>2</sub>Cl<sub>2</sub> under N<sub>2</sub> and stirred at 4°C for 2 hr. *N*-acetylcysteamine (0.12 mmol) was added and the reaction continued for another 24 hr. The reaction mixture was partitioned between 0.1 N aqueous HCl (5 ml) and EtOAc (5 ml), and the aqueous layer was further extracted with EtOAc (25 ml). The organic extracts were washed with saturated NaCl (5 ml), dried (Na<sub>2</sub>SO<sub>4</sub>), and concentrated under reduced pressure to give the polyether-SNAC (50%–60% yield). The colorless oil was directly separated on a silica gel column. CuSO<sub>4</sub>-silica (2 cm) was added to the top of the column to remove the HSNAC. The polyether and derived polyether-SNAC were further purified by preparative RP-HPLC. The formation of each polyether-SNAC derivative was confirmed by MALDI-TOF and MS/MS: *m/z* nanchangmycin (**1**) (M+Na<sup>+</sup>) 889, nanchangmycin-SNAC (**4**) (M+Na<sup>+</sup>) 990; *m/z* nanchangmycin aglycone (**6**) (M+Na<sup>+</sup>) 761, nanchangmycin aglycone-SNAC (**7**) (M+Na<sup>+</sup>) 862; *m/z* monensin (**2**) (M+Na<sup>+</sup>) 693, monensin-SNAC (**5**) (M+Na<sup>+</sup>) 794; *m/z* salinomycin (**3**) (M+Na<sup>+</sup>) 773, salinomycin-SNAC (**8**) (M+Na<sup>+</sup>) 874.

#### TE Activity Assay

For preliminary screening of wild-type and mutant NanE, 10 μM NanE or mutant and 30 μM SNAC-thioester substrate were added to 500 μl of 50 mM phosphate buffer containing 5% methanol, and the mixture was incubated overnight at 30°C. The incubation mixture was extracted twice with ethyl acetate (1 ml) and the concentrated extract was redissolved in 50 μl of methanol. The crude extract was then analyzed directly by MALDI-TOF MS to assay for hydrolysis of the SNAC thioester. A control incubation lacking protein was carried out for each substrate. The matrix consisted of  $\alpha$ -cyano-4-hydroxycinnamic acid in 1:1 (v/v) CH<sub>3</sub>CN and water with 0.1% TFA (1:1). Matrix (3 μl) and sample (3 μl) were mixed, and 1 μl of the mixture was applied to the MALDI-TOF target plate. The standard angiotensin\_linear method (Biospectrometry workstation) was used for direct mass analysis and the angiotensin\_psd method was used for MS/MS analysis.

#### Steady-State Kinetics

##### Diketide-SNAC Hydrolysis

Hydrolysis of diketide-SNAC thioesters **9** and **10** was assayed by reaction of released HSNAC with 5,5'-dithio-2-nitrobenzoic acid (DTNB) and monitoring the formation of 5-thio-2-nitrobenzoate ( $\lambda_{\text{max}} = 412 \text{ nm}$ ;  $\epsilon = 13,600 \text{ M}^{-1} \text{ cm}^{-1}$ ). DMSO was used to solubilize each diketide-SNAC substrate with 500 mM stock DMSO solutions of each of the SNAC thioesters. The reactions (30°C) were monitored at 1 min intervals at 412 nm with a TECAN 96-well plate reader at 412 nm. For incubation of diketide-SNAC **9** and **10** with wild-type NanE, the assay mixture consisted of 50 mM phosphate buffer (pH 8.0), 14 μM NanE,

2.5–50 mM diketide-SNAC, and 20 μl of a saturated solution of DTNB, plus 10% (v/v) DMSO in a total volume of 200 μl. Several parallel control reactions were performed for each substrate, and the data corrected for any background reactions. Controls were as follows: control 1: enzyme and DTNB without substrate; control 2: substrate and DTNB without enzyme; and control 3: only DTNB. Velocities were linear ( $r^2 > 0.98$ ) within the first 10 min. For incubation of NanE mutant W97A with diketide-SNAC **9** or **10**, the assay conditions were the same, except that the concentration of NanE W97A was reduced to 2.8 μM. The data from both sets of assays were fit directly to the Michaelis-Menten equation by nonlinear least-squares regression with Kaleidagraph software to calculate  $k_{\text{cat}}$  and  $K_{\text{m}}$ . Reported standard deviations in the steady-state kinetic parameters represent the calculated statistical errors in the nonlinear, least-squares regression analysis.

##### Hydrolysis of Monensin-SNAC

The preliminary assay mixture consisted of 50 mM phosphate buffer (pH 8.0), 35 μM NanE, **5** at 200 mM or 800 mM, and 10% DMSO in a total volume of 500 μl. The reaction was incubated at 30°C. At intervals of 15, 30, 60, 90, and 120 min, 60 μl samples were withdrawn and quenched by mixing with 20 μl of 1 M HCl. The protein was removed with a 5000 MW cut-off filter (Amicon). Free thiol formation was quantified at 412 nm by mixing 100 μl of a saturated solution of DTNB in 50 mM phosphate buffer (pH 8.0) and 850 μl of 50 mM phosphate buffer (pH 8.0). Steady-state kinetic measurements were carried out in triplicate. Velocity measurements were carried out at concentrations of **5** of 200, 300, 400, 600, and 800 μM. The assay mixtures consisted of 50 mM phosphate buffer (pH 8.0), 35 μM NanE, **5** at various concentrations, and 10% (v/v) DMSO in a total volume of 200 μl. The reactions were incubated at 30°C for 2 hr, conditions under which the reaction had been shown to be linear, at which time three 60 μl samples were quenched by the addition of 15 μl of 1 M HCl. Parallel control reactions were measured at each substrate concentration in the absence of enzyme, and the data were corrected for any background reaction. The average of the normalized data for each triplicate assay was fit to the Michaelis-Menten equation to calculate the  $k_{\text{cat}}$  and  $K_{\text{m}}$ . Reported standard deviations in the steady-state kinetic parameters represent the calculated statistical errors in the nonlinear, least-squares regression analysis.

##### Hydrolysis of Nanchangmycin-SNAC (**4**) and Nanchangmycin Aglycone-SNAC (**7**)

Because nanchangmycin and nanchangmycin aglycone both have strong UV absorbance at 234 nm and are easily resolved by HPLC, the hydrolysis of nanchangmycin-SNAC (**4**) and nanchangmycin aglycone-SNAC (**7**) were each directly assayed by RP-HPLC, monitored at 234 nm with a Phenomenex Synergi 2.5 μm RP C<sub>18</sub> analytical column (100 × 2.00 mm) at a flow rate of 0.4 ml/min. A linear gradient of acetonitrile (solvent B) in water with 0.1% TFA (solvent A) was used to separate each polyether product from the corresponding SNAC-thioester substrate. Separation of nanchangmycin-SNAC (**4**) and nanchangmycin (**1**): 0–3 min, 85% solvent B; 3–7 min, from 85% to 90% solvent B; 7–10 min, 90% solvent B; 10–13 min, from 90% to 95% solvent B; 13–15 min, from 95% to 100% solvent B. Nanchangmycin-SNAC (**4**) retention time was 4.9 min; nanchangmycin (**1**) retention time was 6.8 min. Separation of nanchangmycin aglycone-SNAC (**7**) and nanchangmycin aglycone (**6**): 0–3 min, 60% solvent B; 3–7 min, from 60% to 80% solvent B; 7–10 min, from 80% to 90% solvent B; 10–13 min, from 90% to 100% solvent B; 13–15 min, 100% solvent B. Nanchangmycin aglycone-SNAC (**7**) retention time was 7.2 min; nanchangmycin aglycone (**6**) retention time was 9.8 min. For calibration, a standard curve was generated by integrating the peak area of standard nanchangmycin at a range of concentrations. Assay mixtures consisted of 50 mM phosphate buffer (pH 8.0), 17.5 μM NanE, and variable concentrations of **4** (7.4, 14.85, 29.7, 44.5, and 59.4 μM) and 5% (v/v) methanol in a total volume of 400 μl. The mixtures were incubated at 30°C for 1 hr, conditions under which the reaction had been shown to be linear. They were then extracted with 4 × 300 μl of ethyl acetate, and the combined and concentrated organic extracts dissolved in 20 μl of methanol, and a 10 μl sample was analyzed by HPLC. The initial linear velocities were fit to the Michaelis-Menten equation to calculate  $k_{\text{cat}}$  and  $K_{\text{m}}$ . Reported standard deviations in the steady-state kinetic parameters represent the calculated statistical errors in the nonlinear, least-squares regression analysis. The hydrolysis of nanchangmycin aglycone-SNAC (**7**) (14.5, 29, 58, 116, and 232 μM) was assayed under identical conditions, except that the incubations were carried out for 2 hr, conditions under which the reaction was shown to be linear.

## SUPPLEMENTAL DATA

Supplemental Data include four figures, one table, Supplemental Results, Supplemental Experimental Procedures, and a Supplemental Reference used in this work, and are available with this article online at <http://www.chembiol.com/cgi/content/full/15/5/449/DC1/>.

## ACKNOWLEDGMENTS

This work was supported by National Institutes of Health grant GM22172 to D.E.C., and by grants 973 and 863 from the Ministry of Science and Technology of China, from the National Science Foundation of China to Z.D., and by a studentship from the China Scholarship Council for cotraining Ph.D. program to T.L. We thank Weiguo He for the gift of polyketide-SNAC substrates, Roselyne Castonguay for helpful discussions, Tun-Li Shen for assistance with the mass spectrometric analysis, and Russell Hopson for detailed advice on the NMR analysis. We also thank Rachel Lawson for kind advice on the preparation of the manuscript.

Received: February 13, 2008

Revised: April 4, 2008

Accepted: April 17, 2008

Published: May 16, 2008

## REFERENCES

- Akey, D.L., Kittendorf, J.D., Giraldez, J.W., Fecik, R.A., Sherman, D.H., and Smith, J.L. (2006). Structural basis for macrolactonization by the pikromycin thioesterase. *Nat. Chem. Biol.* **2**, 537–542.
- Aldrich, C.C., Venkatraman, L., Sherman, D.H., and Fecik, R.A. (2005). Chemoenzymatic synthesis of the polyketide macrolactone 10-deoxymethynolide. *J. Am. Chem. Soc.* **127**, 8910–8911.
- Bhatt, A., Stark, C.B., Harvey, B.M., Gallimore, A.R., Demydchuk, Y.A., Spencer, J.B., Staunton, J., and Leadlay, P.F. (2005). Accumulation of an E,E,E-triene by the monensin-producing polyketide synthase when oxidative cyclization is blocked. *Angew. Chem. Int. Ed. Engl.* **44**, 7075–7078.
- Cane, D.E., and Hubbard, B.R. (1987). Polyether biosynthesis. 3. Origin of the carbon skeleton and oxygen atoms of lenoremycin. *J. Am. Chem. Soc.* **109**, 6533–6535.
- Cane, D.E., Liang, T.-C., and Hasler, H. (1981). Polyether biosynthesis. Origin of the oxygen atoms of monensin A. *J. Am. Chem. Soc.* **103**, 5962–5965.
- Cane, D.E., Liang, T.C., and Hasler, H. (1982). Polyether biosynthesis. 2. Origin of the oxygen atoms of monensin A. *J. Am. Chem. Soc.* **104**, 7274–7281.
- Cane, D.E., Celmer, W.D., and Westley, J.W. (1983). A unified stereochemical model of polyether structure and biogenesis. *J. Am. Chem. Soc.* **105**, 3594–3600.
- Fischbach, M.A., and Walsh, C.T. (2006). Assembly-line enzymology for polyketide and nonribosomal peptide antibiotics: logic, machinery, and mechanisms. *Chem. Rev.* **106**, 3468–3496.
- Gallimore, A.R., Stark, C.B., Bhatt, A., Harvey, B.M., Demydchuk, Y., Bolanos-Garcia, V., Fowler, D.J., Staunton, J., Leadlay, P.F., and Spencer, J.B. (2006). Evidence for the role of the monB genes in polyether ring formation during monensin biosynthesis. *Chem. Biol.* **13**, 453–460.
- Gumila, C., Ancelin, M.L., Delort, A.M., Jeminet, G., and Vial, H.J. (1997). Characterization of the potent in vitro and in vivo antimalarial activities of ionophore compounds. *Antimicrob. Agents Chemother.* **41**, 523–529.
- Gust, B., Challis, G.L., Fowler, K., Kieser, T., and Chater, K.F. (2003). PCR-targeted *Streptomyces* gene replacement identifies a protein domain needed for biosynthesis of the sesquiterpene soil odor geosmin. *Proc. Natl. Acad. Sci. USA* **100**, 1541–1546.
- Harvey, B.M., Hong, H., Jones, M.A., Hughes-Thomas, Z.A., Goss, R.M., Heathcote, M.L., Bolanos-Garcia, V.M., Kroutil, W., Staunton, J., Leadlay, P.F., et al. (2006). Evidence that a novel thioesterase is responsible for polyketide chain release during biosynthesis of the polyether ionophore monensin. *ChemBioChem* **7**, 1435–1442.
- Harvey, B.M., Mironenko, T., Sun, Y., Hong, H., Deng, Z., Leadlay, P.F., Weissman, K.J., and Haydock, S.F. (2007). Insights into polyether biosynthesis from analysis of the nigericin biosynthetic gene cluster in *Streptomyces* sp. DSM4137. *Chem. Biol.* **14**, 703–714.
- He, W., Wu, J., Khosla, C., and Cane, D.E. (2006). Macrolactonization to 10-deoxymethynolide catalyzed by the recombinant thioesterase of the picromycin/methymycin polyketide synthase. *Bioorg. Med. Chem. Lett.* **16**, 391–394.
- Khosla, C., Gokhale, R.S., Jacobsen, J.R., and Cane, D.E. (1999). Tolerance and specificity of polyketide synthases. *Annu. Rev. Biochem.* **68**, 219–253.
- Kieser, T., Bibb, M.J., Buttner, M.J., Chater, K.F., and Hopwood, D.A. (2000). *Practical Streptomyces Genetics* (Norwich, UK: John Innes Foundation).
- Liu, T., You, D., Valenzano, C., Sun, Y., Li, J., Yu, Q., Zhou, X., Cane, D.E., and Deng, Z. (2006). Identification of NanE as the thioesterase for polyether chain release in nanchangmycin biosynthesis. *Chem. Biol.* **13**, 945–955.
- Lu, H., Tsai, S.C., Khosla, C., and Cane, D.E. (2002). Expression, site-directed mutagenesis, and steady state kinetic analysis of the terminal thioesterase domain of the methymycin/picromycin polyketide synthase. *Biochemistry* **41**, 12590–12597.
- Nakamura, M., Kunimoto, S., Takahashi, Y., Naganawa, H., Sakaue, M., Inoue, S., Ohno, T., and Takeuchi, T. (1992). Inhibitory effects of polyethers on human immunodeficiency virus replication. *Antimicrob. Agents Chemother.* **36**, 492–494.
- Oliynyk, M., Stark, C.B., Bhatt, A., Jones, M.A., Hughes-Thomas, Z.A., Wilkinson, C., Oliynyk, Z., Demydchuk, Y., Staunton, J., and Leadlay, P.F. (2003). Analysis of the biosynthetic gene cluster for the polyether antibiotic monensin in *Streptomyces cinnamonensis* and evidence for the role of *monB* and *monC* genes in oxidative cyclization. *Mol. Microbiol.* **49**, 1179–1190.
- Otoguro, K., Kohana, A., Manabe, C., Ishiyama, A., Ui, H., Shiomi, K., Yamada, H., and Omura, S. (2001). Potent antimalarial activities of polyether antibiotic, X-206. *J. Antibiot. (Tokyo)* **54**, 658–663.
- Pieper, U., Eswar, N., Davis, F.P., Braberg, H., Madhusudhan, M.S., Rossi, A., Marti-Renom, M., Karchin, R., Webb, B.M., Eramian, D., et al. (2006). MODBASE: a database of annotated comparative protein structure models and associated resources. *Nucleic Acids Res.* **34**, D291–D295.
- Sood, G.R., Robinson, J.A., and Ajaz, A.A. (1984). Biosynthesis of the polyether antibiotic monensin-A. incorporation of [2-<sup>2</sup>H<sub>2</sub>]-, (R)-[2-<sup>2</sup>H<sub>1</sub>]- and (S)-[2-<sup>2</sup>H<sub>1</sub>]-propionate. *J. Chem. Soc. Chem. Commun.*, 1421–1423.
- Sun, Y., Zhou, X., Liu, J., Bao, K., Zhang, G., Tu, G., Kieser, T., and Deng, Z. (2002). '*Streptomyces nanchangensis*', a producer of the insecticidal polyether antibiotic nanchangmycin and the antiparasitic macrolide meilingmycin, contains multiple polyketide gene clusters. *Microbiology* **148**, 361–371.
- Sun, Y., Zhou, X., Dong, H., Tu, G., Wang, M., Wang, B., and Deng, Z. (2003). A complete gene cluster from *Streptomyces nanchangensis* NS3226 encoding biosynthesis of the polyether ionophore nanchangmycin. *Chem. Biol.* **10**, 431–441.
- Tsai, S.-C., Miercke, L.J.W., Krucinski, J., Gokhale, R., Chen, J.C.H., Foster, P.G., Cane, D.E., Khosla, C., and Stroud, R.M. (2001). Crystal structure of the macrocycle-forming thioesterase domain of the erythromycin polyketide synthase: versatility from a unique substrate channel. *Proc. Natl. Acad. Sci. USA* **98**, 14808–14813.
- Tsai, S.-C., Lu, H., Cane, D.E., Khosla, C., and Stroud, R.M. (2002). Insights into channel architecture and substrate specificity from crystal structures of two macrocycle-forming thioesterases of modular polyketide synthases. *Biochemistry* **41**, 12598–12606.
- Tsuji, S.-Y., Cane, D.E., and Khosla, C. (2001). Selective protein-protein interactions direct channeling of intermediates between polyketide synthase modules. *Biochemistry* **40**, 2326–2331.
- Williams, D.R., and Kissel, W.S. (1998). Total synthesis of (+)-amphidinolide J. *J. Am. Chem. Soc.* **120**, 11198–11199.